




## Article

# Chitosan–Starch Films Modified with Natural Extracts to Remove Heavy Oil from Water

Jessica I. Lozano-Navarro <sup>1,2</sup> , Nancy P. Díaz-Zavala <sup>1,\*</sup> , José A. Melo-Banda <sup>1</sup>, Carlos Velasco-Santos <sup>3</sup>, Francisco Paraguay-Delgado <sup>4</sup>, Josué F. Pérez-Sánchez <sup>1</sup> , José M. Domínguez-Esquivel <sup>5</sup>, Edgardo J. Suárez-Domínguez <sup>2</sup> and Jaime E. Sosa-Sevilla <sup>1</sup>

<sup>1</sup> Tecnológico Nacional de México-Instituto Tecnológico de Ciudad Madero, Centro de Investigación en Petroquímica, Prolongación Bahía de Aldair, Ave. de las Bahías, Parque de la Pequeña y Mediana Industria, Altamira 89600, Mexico; yukino\_85@hotmail.com (J.I.L.-N.); melobanda@yahoo.com.mx (J.A.M.-B.); jfperez@live.com.mx (J.F.P.-S.); jaime\_sosa13@hotmail.com (J.E.S.-S.)

<sup>2</sup> Unidad de Posgrado y Educación Continua, Facultad de Arquitectura, Diseño y Urbanismo, Universidad Autónoma de Tamaulipas Campus Sur, Domicilio conocido, Centro Universitario s/n, Universidad Sur, Tampico 89000, Mexico; edgardo.suarez@docentes.uat.edu.mx

<sup>3</sup> Tecnológico Nacional de México-Instituto Tecnológico de Querétaro, División de Estudios de Posgrado e Investigación, Av. Tecnológico s/n esquina Gral. Mariano Escobedo, Col. Centro Histórico, Querétaro 76000, Mexico; cylaura@gmail.com

<sup>4</sup> Centro de Investigación en Materiales Avanzados, S. C., Departamento de Materiales Nanoestructurados, Miguel de Cervantes 120, Complejo Industrial Chihuahua, Chihuahua 31136, Mexico; francisco.paraguay@cimav.edu.mx

<sup>5</sup> Instituto Mexicano del Petróleo, Eje Central Lázaro Cárdenas 152, Ciudad de México 07730, Mexico; jmdoming@imp.mx

\* Correspondence: npatdiaz@hotmail.com; Tel.: +52-833-3574820

Received: 25 October 2019; Accepted: 15 December 2019; Published: 19 December 2019



**Abstract:** Chitosan films were used to remove heavy oil from connate water, deionized water, and seawater. In this research, chitosan–starch films were modified with natural extracts from cranberry, blueberry, beetroot, pomegranate, oregano, pitaya, and grape. These biodegradable, low-cost, eco-friendly materials show an important oil sorption capacity from different water conditions. It was observed that the sorption capacity has a clear correlation with the extract type, quantity, and water pH. In order to understand the physical and chemical properties of the films, they were analyzed according to their apparent density, water content, solubility, and swelling degree by scanning electron microscopy (SEM), thermogravimetric analysis (TGA), gas chromatography–mass spectroscopy (GC–MS), and the determination of surface area using the Brunauer Emmett Teller (BET) method. The results indicate that chitosan–starch films modified with natural extracts can be successfully applied for environmental issues such as oil spill remedy.

**Keywords:** chitosan–starch film; natural antioxidant; green material; oil/water separation; film characterization

## 1. Introduction

The main characteristics of petroleum (crude oil) are its oily consistency and being flammable. Its color range is from dark brown (almost black) to greenish. Petroleum is naturally produced, usually beneath the Earth's surface, from the decomposition of marine animals and terrestrial plants caught under sedimentary materials, at a high temperature and pressure. Chemically, petroleum is a combination of many hydrocarbons in gaseous, liquid, and solid states. It is necessary to consider that the elemental composition of petroleum varies according to the condition of its source. Heavy oil is

very viscous, and hence it hardly flows. The main properties of heavy oil are a high specific gravity and high content of asphaltene, sulfur, nitrogen, and metals (heterocompounds) [1].

Oil spills are related to environment or ecosystem damage, with a corresponding economical loss. In order to solve this problem, oil removal by sorption materials is currently studied by many researchers. The desirable properties of these materials are the low cost\* <sup>NOTE 1</sup>, high efficiency, easy obtaining, and high capacity of sorption; hydrophobicity; high stability; and reusability. One of these promising materials is chitosan [2]. Chitosan is an abundant and natural polymer; it is obtained from the deacetylation of chitin (compound from crustacean shells and bugs exoskeleton). It presents biocompatibility, film forming ability, mechanical strength, and hydrophilicity that allows for its use as an oil/water removal material [3]. Starch is the most abundant natural polymer; in recent decades, it has been studied as a material for food packaging and preservation. Because of its properties, starch can be combined with other natural polymers, it is a key material for composite synthesis [4]. Chitosan films are used not only in antimicrobial and packaging applications, but also on crude oil removal. In recent years, the investigation of modified chitosan as an oil removal material has been successfully developed. Doshi et al. (2017) used N,O-carboxymethyl chitosan to remove hydrocarbons from water resources by an adsorption mechanism, and analyzed the influence of pH solution, salinity, and N,O-carboxymethyl chitosan (NO-CS) dosage on the adsorption capacity [5]. Li et al. (2018) used chitosan modified with oxidized cellulose hydrogel, which exhibited lipophilicity, hydrophobicity, and also a high absorption capacity for crude oil and organic solvents, such as ethylene glycol, ethyl acetate, ethanol, and acetone. [3]. There are other green materials used as biosorbents. Luo et al. (2019) synthesized microcrystalline cellulose (MCC) aerogels, with high amylose corn starch and a NaOH–urea solution, which presented an optimum absorption ratio [6]. Long et al. (2019) analyzed the absorption capacity of aerogels created using cellulose, montmorillonite, and a solution of sodium hydroxide and urea, obtaining absorption capacities similar to commercial propylene absorbents [7]. Wang et al. (2019) demonstrated that hydrophobic alginate-based foams induced by zirconium ions showed excellent adsorption capacities for different oils and organic solvents [8].

The main aim of this research was to develop effective oil sorbent materials based on chitosan and starch, modified with natural extracts from cranberry (*Vaccinium oxycoccus*), blueberry (*Vaccinium myrtillus*), beetroot (*Beta vulgaris*), pomegranate (*Punica granatum*), oregano (*Origanum vulgare*), pitaya (*Hylocereus undatus*), and resveratrol or 3,5,4'-trihydroxystilbene from grape (*Vitis vinifera*), and to characterize them in order to understand the relationship between their oil sorption capacity and their properties. These extracts contain several phenolic compounds, such as carboxylic acids and antioxidants (anthocyanins, betalains, carvacrol, resveratrol, and thymol). The results obtained by the material's sorption capacity test allow for knowing which extracts are more suitable for the analyzed application. The films were analyzed using scanning electron microscopy (SEM), determination of surface area by the Brunauer Emmett Teller (BET) method, gas chromatography–mass spectroscopy (GC–MS), and thermogravimetric analysis (TGA). Other analyses were the water pH measurement, apparent density, and physical properties (water content, soluble mass, and swelling degree) of the films. According to the results, these materials are efficient in removing oil from connate water, deionized water, and seawater; this capacity is higher in modified films with natural extracts in comparison with the control chitosan–starch (QS2) film. The sorption capacities obtained in this research were compared with those presented by other green materials, in order to know the viability of using these modified materials. It was found that they are promising candidates as removal materials, because of their oil affinity and high oil sorption capacity, with several advantages such as simpler and more economic synthesis, easy handling, sustainability, biodegradability, environmental-friendly character, and non-toxicity.

## 2. Materials and Methods

### 2.1. Materials and Reagents

Chitosan from shrimp with a medium molecular weight (190,000–310,000 Da) and a degree of deacetylation of 85%, and rice starch were purchased from Sigma-Aldrich (Toluca, Estado de Mexico, Mexico). Glacial acetic acid, glycerol, and deionized water were bought from Fermont (Monterrey, Nuevo León, Mexico). Blueberry, beetroot, and pitaya extracts were obtained from raw pulp fruits at 25 °C, and were filtered before being added to the matrix blend. The aqueous oregano extract was prepared at 5% (*w/v*) using dry oregano and water as a solvent, and the solution was heated at 65 °C for 10 min, with magnetic agitation and further filtration. Commercial organic cranberry and pomegranate juices were used and filtered at 25 °C before their addition to the blend. Resveratrol capsules were purchased from General Nutrition Centers (Pittsburgh, PA, USA). The aqueous resveratrol solution at 5% (*w/v*) was prepared at 25 °C after it was filtered. The obtaining of extracts at room temperature was determined (except in the case of obtaining of oregano extract) to preserve their antioxidants, because of their high temperature sensibility [9–12]. These types of extracts allowed for a reduction of expenses and avoiding toxic solvents, and they were compatible with the film matrix. The crude oil with an API gravity of 12° (American Petroleum Institute) and its connate water was obtained from Aguacate well 20, located in Naranjos, Veracruz, Mexico, and it was proportionated by Petróleos Mexicanos (PEMEX). The seawater was collected from Playa Miramar, Tamaulipas, Mexico.

### 2.2. Synthesis of Films

The chitosan solution (2%, *w/v*) was prepared using a glacial acetic acid solution (1%, *v/v*). The resulting blend was stirred for 24 h at room temperature. A rice starch solution (2% *w/v*) was prepared by heating at  $90 \pm 2$  °C for 20 min, with constant stirring. The solution was cooled to approximately 25 °C. The film formation was carried out using 40 mL of the chitosan solution and 40 mL of the rice starch solution. Subsequently, 0.2 mL of glycerol was added as a plasticizer. Each film blend was stirred for 5–10 min, and later, the resulting blend was verted in a polystyrene tray. Finally, the films were dried at 25 °C for 15 days [13]. For the films with natural extracts, two fixed quantities (0.4 and 1.6 mL) of each extract were added into the polymer solution (corresponding to 0.5% and 2% of the total blend weight). Fifteen films were prepared, as follows: one control film (QS2) and fourteen films with natural extracts (two films for each extract). The significance of the code used for films is given below Table 1.

### 2.3. Physical Properties: Water Content, Soluble Mass, and Swelling Degree

The water content, soluble mass, and swelling degree of the films (without crude oil) were determined using modifications of the processes used by Souza et al. (2017) [14]. The water content analysis is not only useful to know the films' moisture, but also to avoid or reduce the inaccuracy of the soluble mass and the swelling degree results. The purpose of studying the swelling degree and soluble mass is to determine the hydrophobic/lipophilic film character. Also, a higher water-soluble mass may enhance the film biodegradability [15]. To carry out the tests, samples were cut in a quadrangular form (1 × 1 cm) and weighed using an analytical balance model Pioneer, brand OHAUS (Parsippany, NJ, USA). This value is known as the initial weight ( $M_1$ ). Subsequently, the samples were dried in a conventional oven model Lab Line, brand Thermo Scientific (Waltham, MA, USA) at 70 °C for 24 h so as to obtain the initial dry mass value ( $M_2$ ). After that measurement, the film samples were placed in a vial containing 15 mL of deionized water, the vials were capped and left to stand for 24 h at room temperature (about 25 °C). Later, the remaining water (not sorbed by the film samples) was discarded, and the samples were dried using an absorbent paper and then weighed ( $M_3$ ). The samples were dried in the same oven at 70 °C for 24 h in order to determine the final dry mass ( $M_4$ ). The tests were carried out in triplicate, and the average values of the parameters were calculated and are expressed as results

in Table 1. The water content, soluble mass of the film, and degree of swelling were calculated by the following Equations (1)–(3):

$$\text{Water content, \%} = ((M_1 - M_2)/M_1) \times 100 \quad (1)$$

where

$M_1$  = Initial weight, g

$M_2$  = Initial dry mass, g

$$\text{Soluble mass, \%} = ((M_2 - M_4)/M_2) \times 100 \quad (2)$$

where:

$M_2$  = Initial dry mass, g

$M_4$  = Final dry mass, g

$$\text{Swelling degree, \%} = ((M_3 - M_2)/M_2) \times 100 \quad (3)$$

where:

$M_3$  = Sample mass after superficial drying with filter paper, g

$M_2$  = Initial dry mass, g [14].

#### 2.4. pH Measurement of Water

The pH tests were carried out to relate the film sorption capacity with the acidity of the water where the crude oil is located, at standard conditions (25 °C and atmospheric pressure). For this measurement, a pH measuring device, model SM-38W Microprocessor, brand Science MED (Lakeway, TX, USA), was used. The tests were carried out in triplicate, in a room with controlled conditions of temperature (25 °C). The average pH values were expressed as results, and they are indicated in Table 2.

#### 2.5. Removal of Heavy Oil from Connate/Deionized/Seawater Mixtures (Sorption Capacity)

The removal experiment was carried out using known amounts of connate or deionized or seawater (80 mL) and crude oil (1.5 g approximately). Then, quadrangular film samples measuring  $0.7 \times 0.7$  cm were placed on the surface of the oil/water mixture. The contact time between the film samples and the water/oil mixture was 15 min. The film samples were weighed before and after the crude removal process. This operation was repeated three times for each film. The results are reported as an average value in Table 3. The sorption capacity for each case was calculated using Equation (4), as follows:

$$q_t = (m_t - m_0)/m_0 \quad (4)$$

where:

$q_t$  = Sorption capacity at a given time, g/g

$m_t$  = Mass of the impregnated material (weight of the film and the sorbed hydrocarbon), g

$m_0$  = Mass of the sorbent material (weight of the film), g [2,6–8].

#### 2.6. Scanning Electron Microscopy (SEM)

The morphology of the dry films with and without sorbed crude oil was studied using a cold FEG (Field Emission Gun) field emission scanning electron microscope, model JSM-7401F, brand JEOL (Peabody, MA, USA). A piece of each sample was held by a carbon strip. The images were acquired at a low voltage 2 kV, to avoid electron charging, and a magnification of 1700× was made for each sample. To hold each sample, a carbon strip was used during the analysis.

## 2.7. Thermogravimetric Analysis (TGA)

This analysis was performed to determine the thermal stability of the films, for this purpose the best sorbent materials were selected (0.5% extract concentration). Also, from this information, the application in oil/water mixtures at high temperatures before material degradation can be presumed. A TGA analysis of the samples was performed using a thermogravimetric analyzer model TGA SDT Q600 V20.9 Build 20, brand TA Instruments (New Castle, DE, USA), with 50.0 mL/min airflow and a heating rate of 10 °C/min from room temperature to 600 °C. The starting sample weight was between 8 and 30 mg. The TGA results are indicated in Tables 4 and 5.

## 2.8. Apparent Density

The apparent density is inversely related to the porosity (pore space). To determine this property, a modified procedure by Ahmed et al. [16] was used. The film samples were cut in a circular shape and later they were weighed. For this test, an analytical balance model Pioneer, brand OHAUS (Parsippany, NJ, USA) was used. Other parameters such as the diameter and height were considered. The apparent density ( $\rho$ ) was obtained by Equation (5), as follows:

$$\rho = W / [\pi \times (D/2)^2 \times H] \quad (5)$$

where:

$\rho$  = Apparent density

D = Sample diameter

H = Sample height

W = Sample weight [16]

The average apparent density results are indicated in Table 6.

## 3. Results and Discussion

### 3.1. Physical Properties: Water Content, Soluble Mass, and Swelling Degree

The physical properties of the removal materials, such as the water content %, soluble mass %, and degree of swelling % were analyzed. The results are indicated in Table 1, and compared with those obtained by control film QS2. In these tests, it was indicated that the water content (%) is higher in 3 of 14 films. In analyzing the soluble mass % results, it was observed that the soluble mass values are in a range of approximately 18–44%, also an increment of soluble mass was observed in 9 of 14 films. In the swelling degree (%) tests, it was observed that only 4 of 14 films have a higher value.

**Table 1.** Physical properties of films: water content (%), soluble mass (%), and swelling degree (%).

Sample <sup>1</sup>	Average Water Content (%)	Average Soluble Mass (%)	Average Swelling Degree (%)
QS2	14.46 ± 5.88	20.63 ± 2.78	88.25 ± 2.10
QSA0.5	9.81 ± 0.63	21.77 ± 3.44	57.94 ± 0.15
QSA2	13.47 ± 4.46	29.07 ± 1.47	82.70 ± 7.43
QSAm0.5	14.05 ± 4.67	24.39 ± 6.45	34.63 ± 17.36
QSAm2	12.83 ± 4.31	18.95 ± 3.67	38.51 ± 15.77
QSB0.5	15.09 ± 5.02	19.75 ± 2.44	79.26 ± 10.17
QSB2	11.98 ± 2.29	21.67 ± 4.59	38.89 ± 29.97
QSG0.5	11.93 ± 1.71	16.48 ± 1.53	100.45 ± 7.89
QSG2	12.94 ± 2.20	35.29 ± 19.94	68.73 ± 5.82
QSO0.5	10.80 ± 0.59	18.99 ± 0.66	90.13 ± 0.70
QSO2	13.04 ± 3.30	23.27 ± 4.01	81.73 ± 3.38
QSP0.5	18.02 ± 1.66	44.27 ± 12.56	27.55 ± 22.99
QSP2	13.19 ± 5.67	30.63 ± 13.30	70.13 ± 4.09
QSR0.5	17.17 ± 4.09	20.72 ± 0.03	95.25 ± 4.03
QSR2	11.88 ± 1.24	18.44 ± 3.57	149.29 ± 5.72

<sup>1</sup> Q—chitosan; S—starch; A—cranberry; Am—blueberry; B—beetroot; G—pomegranate; O—oregano; P—pitaya/dragon fruit; R—resveratrol; numbers refer to the weight percentage of the extract used in each film.

According to Souza et al. (2017), the increment of water content in chitosan films modified with essential oils and hydro-alcoholic extracts could be due to presence of aromatic rings and phenolic compounds [14]. The addition of resveratrol increased the water content of the QSR0.5 film, this fact coincides with the report presented by Pastor et al. (2013) [17]. The increment of water content % is observed films with beetroot, pitaya, and resveratrol at 0.5%, the rest of the films presented a decrement in these values.

The study of the soluble mass (%) is very important, because high soluble mass values indicate less water resistance. The lower soluble mass % in the films with extracts was above 16%. The soluble mass increment is related to the addition of extracts (except for pitaya films, this could be attributed to the presence of its betalains), no matter the extract's concentration. This agrees with the results of Wang et al. (2013), who showed that the addition of tea polyphenols increases the film soluble mass [18]. A soluble mass below 25% could be optimal in order to preserve the film stability (Blanquicet-Macea et al. (2015) observed that soluble mass of chitosan/whey films was in order to 7–24%) [19]. According to Mayachiew and Devahastin (2010), the decrement of the swelling degree is due to the presence of natural extracts (in their case, Indian gooseberry extract). The interaction between chitosan and extract, and the hydrophobic behavior allowed for this decrement [20]. The hydrophobic interaction between the polyphenols and the chitosan hydrophobic regions causes the blocking of certain active groups for water adsorption, which results in a decrement of the swelling degree in films. A hydrophobic interaction was observed more intensely in QSA<sub>m</sub>2 (lower swelling degree and lower soluble mass). No hydrophobic interaction was observed more intensely in QSR0.5 (an increment of swelling degree is observed and the decrement of soluble mass is not presented) [21]. A high degree of deacetylation of chitosan is related to a higher rate of swelling, as the content of the amino group increases. The amino group -NH<sub>2</sub> is hydrophilic (highly related to water). It was observed that the addition of natural extracts, in most cases, reduced the degree of swelling of the films, compared with QS2. This may be because the polar groups and the water in the extracts generate weaker hydrogen bonds than those created between the hydroxyl and amino groups (coming from the matrix of the film, namely: chitosan, starch, and glycerol), which results in the swelling reduction [19].

These results mean that films with a lower water content could show a longer shelf life and a wider range of applications as their biodegradability is lower in comparison with control film QS2. The increase in the soluble mass of the materials could only affect the application of these if it occurs in combination with a high water content %. The decrease in the degree of swelling is related to the interaction of the chitosan and antioxidants (polyphenols) present in the extracts, which is related, at the same time, with the hydrophobic properties of these materials, allowing for the correct removal of crude from the water. The chemical interaction between the chitosan and antioxidants varied due to the film composition. It was also observed that this material always remained afloat and quickly adhered to the crude.

### 3.2. pH Measurement of Water

The different sources of water were analyzed to know whether the pH value affects the sorption capacity of films. The pH of the different types of water does not differ greatly, the order of lowest to highest pH value is deionized water < congenital water < seawater; these results can be observed in Table 2.

**Table 2.** pH values of connate water, deionized water, and seawater.

Sample	Test 1	Test 2	Test 3	Average pH
Connate water	6.8	6.81	6.81	6.81 ± 0.006
Deionized water	6.67	6.67	6.7	6.68 ± 0.017
Seawater	7.53	7.5	7.51	7.51 ± 0.015



Correlating the sorption capacity results shown in Table 3 and the pH data from Table 2, it was found that the best sorption capacity is present in seawater (highest pH), followed by deionized water (lowest pH), and finally connate water (which has a medium pH value). At lower pH values (deionized water) it is more effective to use films with concentrations of 2% (v/v), and for higher pH values (deionized water and seawater) the use of materials with concentrations of 0.5% (v/v) is more effective.

A similar relationship between the pH media and oil removal was observed by Saruchi et al. (2016), who synthesized an interpenetrating polymeric network from natural polysaccharides and used it under three different pH conditions (pH = 3, 7, and 10). The research results showed that the higher sorption happened at pH = 3, the medium sorption at pH = 10, and the lower sorption at pH = 7 [22]. A higher sorption capacity can be related to a strong acid condition, which leads to unstable folk formation. The acid condition of the sample acted as a “catalyzer” in the reaction between a crude molecule and the material sorption sites. The effective oil removal does not mean that these materials do not present a sorption capacity in alkaline or neutral conditions (in these cases, the expected sorption capacity is lower). Also, the sorption or oil removal capacity is highly dependent on the sorbate extract concentration. This is confirmed by the research of Rongsayamanont et al. (2017), who indicated the stability of biosorbents (composed by lipopeptides, glycerol, and palm oil) at a pH media range of 4–10 (using substances such as deionized water, alkaline water at pH 9, methanol, ethanol, dimethyl sulfoxide, acetone, chloroform, and hexane, it pointed the sorption capacity of biomaterials in acidic and alkaline media) without losing the film stability [23]. It is important to remark that the addition of higher quantities of extract gives the materials a lower pH value [13]. This fact allows the films to have a higher affinity and effectivity in acid media.

### 3.3. Removal of Heavy Oil from Connate/Deionized/Seawater Mixtures (Sorption Capacity)

The removal action of the chitosan–starch modified films was proved using three oil/water mixtures using connate water and heavy oil from Aguacate well (1); deionized commercial water and heavy oil from Aguacate well (2); and seawater from Playa Miramar, Madero City, Tamaulipas, and oil from Aguacate well (3). In Figure 1, the procedure of oil removal from water by the sorption capacity of modified films is shown. The results obtained in these tests are indicated in Table 3.

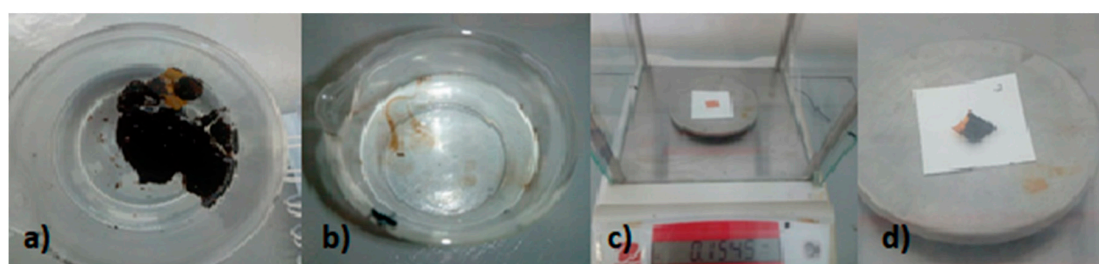


**Figure 1.** Oil removal from water using modified chitosan–starch films: (a) oil/water with film samples, (b) water after removal process, (c) film sample, and (d) film sample with oil.

**Table 3.** Average sorption capacity ( $q_t$ ) of the films.

Sample	Average Sorption Capacity ( $q_t$ ), g/g		
	Oil/Connate Water	Oil/Deionized Water	Oil/Seawater
QS2	$8.73 \pm 3.87$	$7.78 \pm 2.32$	$7.05 \pm 2.22$
QSA0.5	$13.44 \pm 2.70$	$7.65 \pm 3.82$	$19.69 \pm 3.15$
QSA2	$3.62 \pm 1.82$	$23.85 \pm 5.01$	$7.99 \pm 3.32$
QSA0.5	$18.43 \pm 2.12$	$12.93 \pm 2.10$	$20.22 \pm 4.30$
QSA0.5	$1.71 \pm 1.46$	$10.88 \pm 1.39$	$8.61 \pm 2.26$
QSB0.5	$11.74 \pm 3.77$	$11.21 \pm 3.62$	$16.96 \pm 2.84$
QSB2	$8.35 \pm 2.61$	$21.01 \pm 12.93$	$8.63 \pm 2.29$

Table 3. Cont.

Sample	Average Sorption Capacity ( $q_t$ ), g/g		
	Oil/Connate Water	Oil/Deionized Water	Oil/Seawater
QSG0.5	10.91 ± 3.17	9.33 ± 0.69	8.81 ± 1.76
QSG2	6.14 ± 2.86	19.50 ± 6.32	6.58 ± 2.89
QSO0.5	10.50 ± 4.78	14.41 ± 0.72	12.33 ± 1.09
QSO2	5.80 ± 5.10	11.20 ± 3.17	12.24 ± 1.16
QSP0.5	23.55 ± 6.33	7.93 ± 0.42	11.09 ± 2.34
QSP2	11.73 ± 7.26	17.44 ± 0.103	6.09 ± 1.62
QSR0.5	19.73 ± 3.25	7.38 ± 0.99	10.58 ± 2.82
QSR2	2.79 ± 3.49	13.00 ± 1.56	8.21 ± 4.20

Also, the obtained results are described below.

Removal of oil from connate water (1): Observing the results obtained from the removal tests, we can conclude that the addition of natural extracts in the lowest concentration (0.5% *v/v*) increases the sorption capacity of the materials in comparison with the control film QS2 and the modified films with higher quantity of extracts (except for QSP2), especially in the case of cranberry, blueberry, pitaya, and resveratrol extracts. Of the 14 modified chitosan films, 8 presented a higher sorption capacity compared with the control film (QS2; see Table 3). The film with the highest sorption capacity for this case is QSP0.5.

Removal of oil from deionized water (2): According to the results of Table 3, most of the films presented a higher sorption capacity than the control film QS2; this behavior could be attributed to the addition of natural extracts. The best results were observed in most cases (except blueberry and oregano) when the extracts are present in a concentration media (2% *v/v*). The film with the highest sorption capacity for this case is QSA2. The synthesized materials showed a better oil sorption capacity when the crude oil was emulsified with deionized water than with connate water. Of the 14 materials, 12 have higher sorption capacity values compared with the control film QS2 (see Table 3).

Removal of oil from seawater (3): Table 3 shows the effect of the addition of natural extracts on the increment of the sorption capacity of modified films in comparison with control film QS2. Of the 14 modified films, 12 presented this behavior (see Table 3). The best results of each extract were observed for the lowest concentration (0.5% *v/v*). The films with the highest sorption capacity for this case are QSA0.5 and QSA0.5.

The results point out that the materials presented a better performance in deionized water (potable) and seawater than in connate water. The increment in the oil sorption capacity of the modified films is due to the hydrophobic interaction between chitosan and antioxidants (polyphenols). This implies that despite the swelling degree %, these materials have a greater affinity with oil than with water. The chemical interaction between chitosan and antioxidants varies due to the film composition. The type of extracts and their concentration in films has an influence on the sorption capacity (lowest concentrations and the use of blueberry, beetroot, pomegranate, and oregano enhance this capacity)\* NOTE 2. In Figure 2b, the best sorption capacity occurs using 0.5% (*v/v*) of extracts; this means that the lower the extract concentration, the higher the average sorption capacity. A similar behavior was obtained by Saruchi et al. (2016), who synthesized an interpenetrating polymer network (IPN) of gum tragacanth, poly acrylic acid (PAA), and poly acrylamide (PAAm) for oil removal from water; the pH of the water that contains the crude oil is a factor that influences the removal of crude. In Figure 2a, the relationship between the pH values and the total average oil sorption capacity coincides with what is stipulated by them—at the lowest pH this value increases, a decrement was observed at a medium pH, and an increment was observed at the highest pH. Also, they found that the use of a low quantity of sorbent (corresponded to 0.002 weight % of the oil/water mixture in their case, and 0.003 % in this study) can show optimal oil sorption results [22].



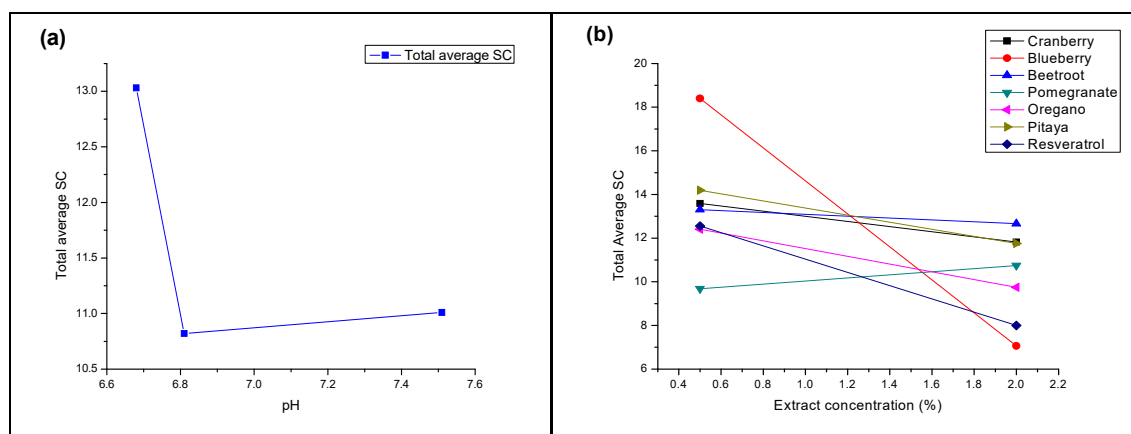


**Figure 2.** Effect of the (a) pH of water in mixture; (b) type and concentration of extracts on the sorption capacity of chitosan–starch films.

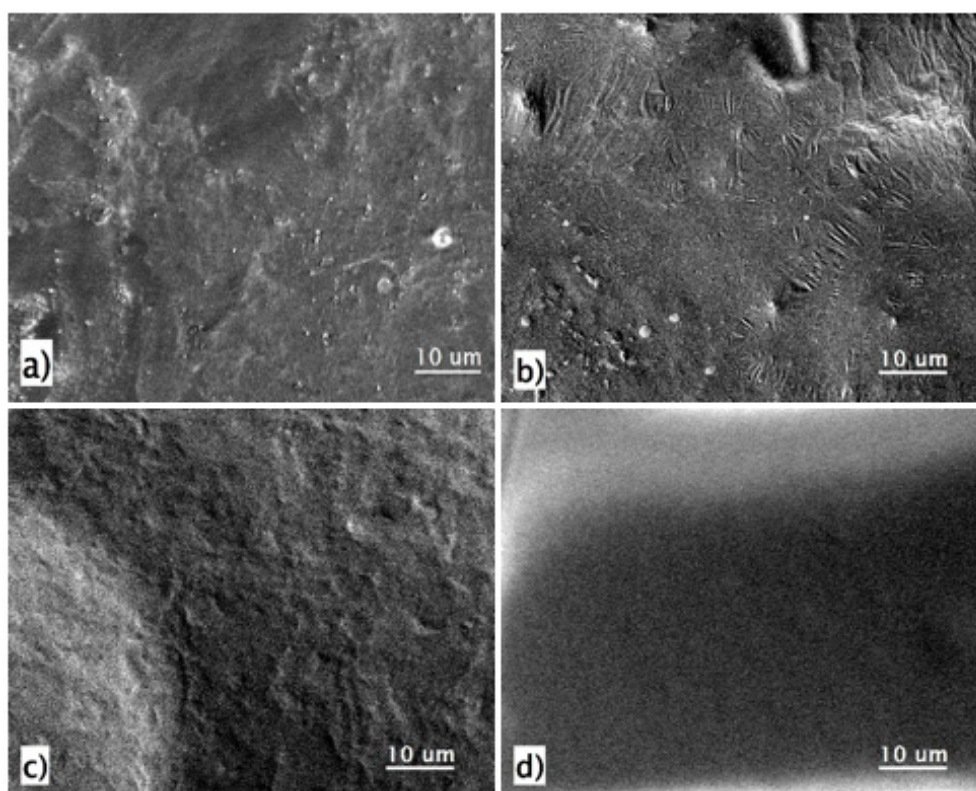
In order to know the viability of these newly synthesized materials, their sorption capacity results were compared with those obtained by some researchers in recent dates. Li et al. (2018) used chitosan/cellulose aerogel as an oil removal material for different kinds of oil. They obtained sorption capacities between 14.67–18.90 g/g [2]. Luo et al. (2019) used high amylose cornstarch–microcrystalline cellulose aerogel. They obtained a sorption ratio of 7.97–10.63 g/g for vacuum pump oil and 8.98–11.44 g/g for linseed oil, and the highest results were presented by the samples with a medium starch concentration [6]. Long et al. (2019) synthesized cellulose aerogels with sodium montmorillonite, and showed a sorption capacity between 4.5 g/g and 6 g/g for #48 and #220 lubricating oil [7]. Wang et al. (2019) used hydrophobic alginate-based foams induced by zirconium ions for oil and organic solvents cleanup, and obtained a sorption capacity of 3.3–28.9 g/g [8]. Comparing the results obtained by other researchers with those presented in Table 3, it was observed that most of the sorption capacity tests (43 of 45) showed values above 3 to almost 25 g/g; the best results were achieved by the films with a 0.5% extract concentration. That indicates that the materials of chitosan–starch with natural extracts are promising candidates for further oil removal investigation, because of their adequate sorption capacity.

### 3.4. Scanning Electron Microscopy (SEM)

The films with a 0.5% extract concentration were analyzed by SEM to determine if a relationship between their morphology and their higher sorption capacity exists. The micrographs from Figure 3 to Figure 5 show images for samples QS2, QSAm0.5, QSB0.5, QSG0.5, QSO0.5, and QSR0.5, respectively. These images were all acquired at 1700× magnification. Figures 3a,c, 4a,c and 5a,c are from the samples before the oil absorption capacity experiments, and Figures 3b,d, 4b,d and 5b,d are from the samples after the oil adsorption capacity experiments. The white spots zones in the film surfaces are related to the rice starch, which was used for blending with the chitosan. Table 4 shows details of the films' morphology explanation. The images from some films with oil adsorption showed a brighter surface (white) in comparison with those without oil adsorption. In these zones, it is not from the electron charge during the images acquisition; if it is, the image should show a drift.

**Table 4.** Film's morphology before and after the oil sorption capacity test.

Film	Morphology before Sorption Capacity Test	Morphology after Sorption Capacity Test
QS2	A more homogenous surface in comparison with the modified films, few streaks, and very tiny white spots.	A thin oil layer on the film surface gives it a rough appearance with streaks that change the film morphology visualization.
QSA0.5	Heterogeneous films surface with the presence of convexities and very few tiny white spots.	Thick, smooth layer, due to the exposure oil on the film surface that hinders the film's morphology visualization.
QSB0.5	The film surface has some streaks, convexities, and concavities; also, there is presence of a few tiny white spots.	Thick oil layer on the film surface, it was more remarkable in the convexity/concavity zones, and the presence of starch is still visible.
QSG0.5	Presence of convexities and a few white points, there are no streaks.	Smoothing of film morphology, a more homogenous aspect, and the white point cannot be observed, and there are imperfections (wrinkled).
QSO0.5	Homogenous film surface with a few convexities and multiple points due to starch.	The starch presence is more noticeable in this case; a less oil sorption can be inferred.
QSR0.5	Morphology surface with streaks, some white points.	The oil forms a layer on the surface that smooth the film morphology.

**Figure 3.** Micrographs from sample QS2: (a) before oil exposure and (b) after crude oil exposure both at 1700×; from sample QSA0.5 (c) before oil exposure and (d) after oil exposure, both at 1700×.

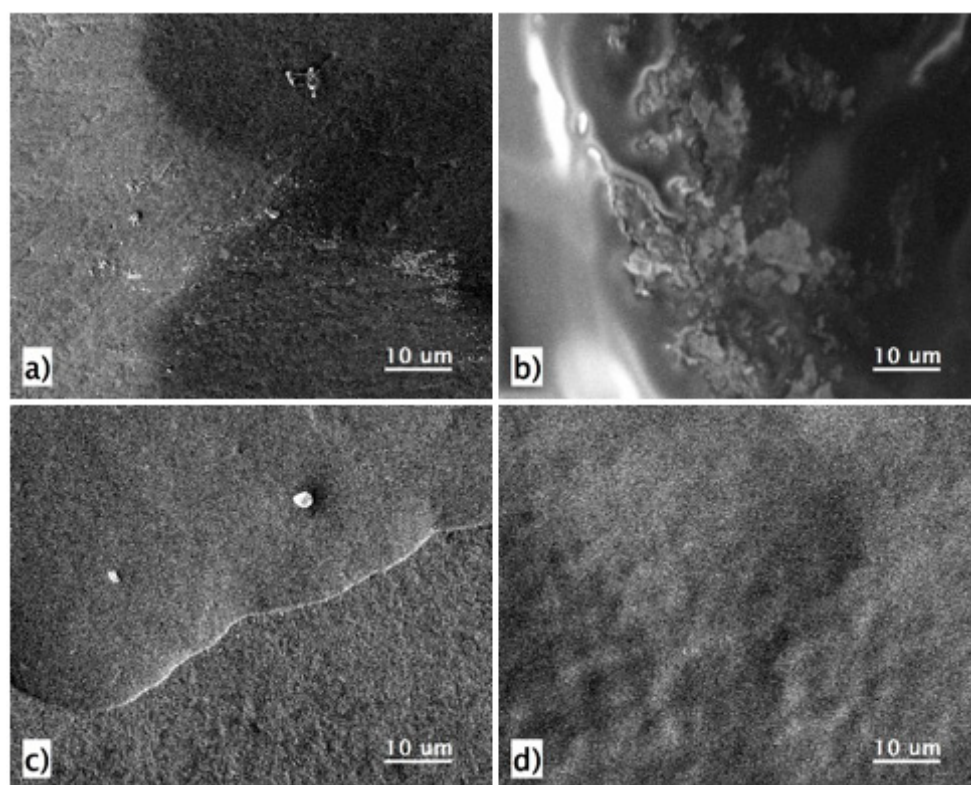


**Figure 4.** Micrographs from sample QSB0.5: (a) before oil exposure and (b) after crude oil exposure, both at 1700 $\times$ ; from sample QSG0.5 (c) before oil exposure and (d) after oil exposure, both at 1700 $\times$ .

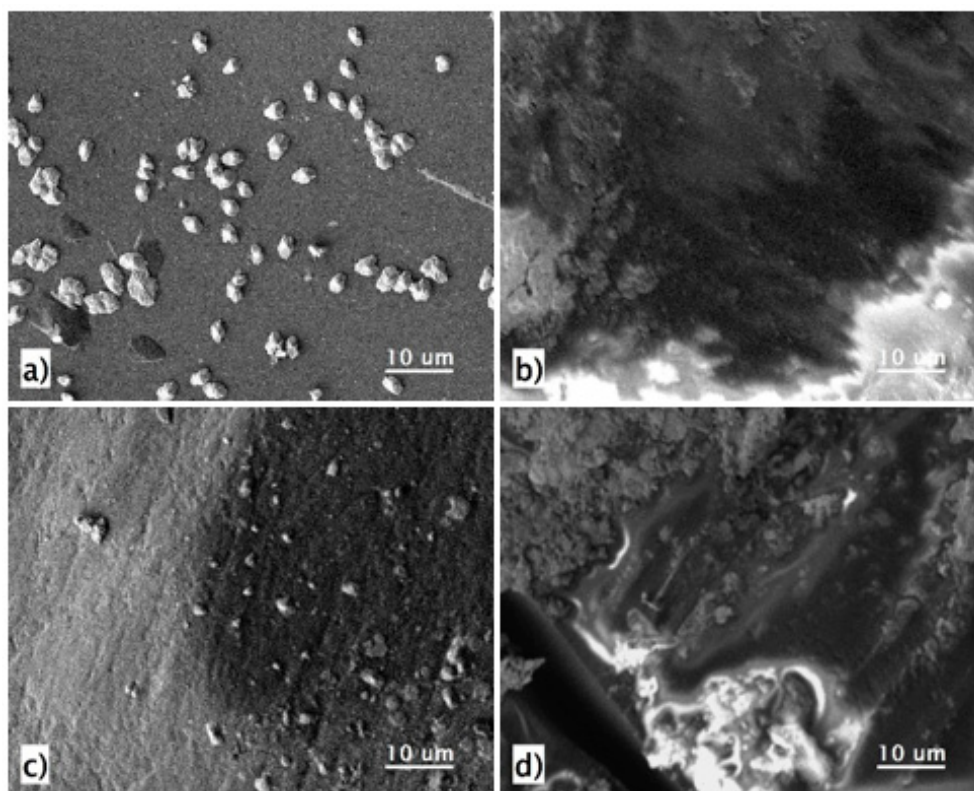


**Figure 5.** Micrographs from sample QSO0.5: (a) before oil exposure and (b) after crude oil exposure, both at 1700 $\times$ ; from sample QSR0.5 (c) before oil exposure and (d) after oil exposure, both at 1700 $\times$ .

According to Elanchezhiyan and Meenakshi (2017), the heterogeneous film surfaces improve the oil sorption capacity through the diffusion of oil particles on to the surface of the sorbent material. Also, they observed that after oil removal, the surface heterogeneity was smoothed because of the oil molecules' occupation on the sorbent surface [24].

According to Doshi et al. (2018) and Lozano et al. (2018), the chitosan morphology modification and the surface roughness increment are due to the addition of some components such as carboxymethyl or natural extracts. The presence of more complex components (with higher molecular weight), such as anthocyanins and betalains, causes a rougher surface in comparison with the thymol and carvacrol antioxidants (present in oregano extract) and the control film QS2 [25,26]. The addition of compounds modifies the homogeneity of the film's surface and causes the "aggregated" appearance in the polymer matrix; Noshirvani et al. (2017) observed a similar behavior using oleic acid [27].

Comparing the SEM micrographs with the oil removal results, a higher oil removal implies a higher oil sorption, and the formation of a thicker oil slay on film surface that smooths/conceals the original morphology visualization. This relationship was clearer in the case of QSA0.5, QSB0.5, and QSG0.5, which presented some of the highest oil sorption capacities in the three types of oil/water mixtures. The presence of white points due to starch do not significantly affect the oil sorption capacity (QSO0.5 and QSR0.5 films). Concavities and streaks on the film's surface are related to a significant oil sorption capacity increment due to a wider surface area for the sorption phenomena.

### 3.5. Thermogravimetric Analysis (TGA)

The films with a 0.5% extract concentration were analyzed by TGA to study the relationship between their thermal stability and their higher sorption capacity. The thermal degradation of the samples QS2, QSA0.5, QSA0.5, QSB0.5, QSG0.5, QSO0.5, QSP0.5, and QSR0.5 were analyzed by thermogravimetric analysis. The thermograms are shown in Figure 6. Three weight losses or thermal events across each TGA curve were observed, which are described in Table 5.

**Table 5.** Weight loss percentage at 135, 320, and 600 °C for each film.

Temperature Range of Weight Loss	Thermal Events Related to the Weight Loss
First weight loss: room temperature (135 °C)	Removal of moisture and volatile materials. The degradation of the antioxidants (except resveratrol) should occur at the end of this weight loss.
Second weight loss: (135–320 °C)	Decomposition of the chitosan into amino units and the plasticization of starch. Resveratrol decomposition starts at 240 °C, approximately. Decomposition of glycerol (at 290 °C approximately)
Third weight loss (320–600 °C)	Decomposition of the –CHOH group. Total degradation of the chitosan and starch cyclic structures arises at 600 °C.

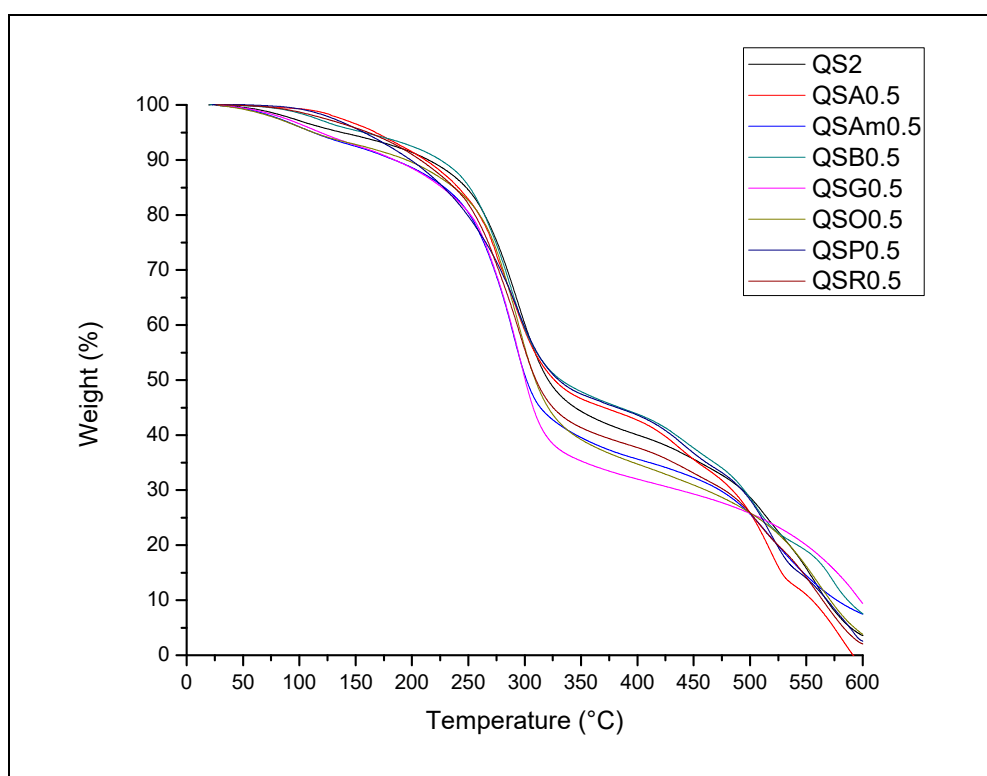
A greater displacement at the end of the curve of film QSA0.5 was observed, in comparison with the rest of the samples. This displacement could seem like an expected behavior when blueberry extract is used, which could indicate a greater plasticization in this kind of material. Observing the beginning of all of the TGA curves, it was found that all have the same characteristics because of the acetylation of the material, except for QSO0.5. This kind of behavior can be attributed to the presence of thymol and carvacrol from the oregano extract [25,28–32]. Table 6 shows the weight loss percentages of each film at 135, 320, and 600 °C.



**Table 6.** Weight loss percentage at 135, 320, and 600 °C of each film.

Sample	Weight Loss Percentage at 135 °C	Weight Loss Percentage at 320 °C	Weight Loss Percentage at 600 °C
QS2	4.88 ± 0.20	49.72 ± 0.20	96.47 ± 0.20
QSA0.5	2.34 ± 0.20	48.49 ± 0.20	100.00 ± 0.20
QSA0.5	6.63 ± 0.20	56.35 ± 0.20	92.56 ± 0.20
QSB0.5	3.87 ± 0.20	47.70 ± 0.20	92.50 ± 0.20
QSG0.5	6.30 ± 0.20	60.40 ± 0.20	90.62 ± 0.20
QSO0.5	6.45 ± 0.20	54.76 ± 0.20	96.24 ± 0.20
QSP0.5	2.89 ± 0.20	47.79 ± 0.20	97.46 ± 0.20
QSR0.5	3.22 ± 0.20	53.68 ± 0.20	95.96 ± 0.20

The lowest total weight loss (at 600 °C) is presented by the QSA0.5, QSB0.5, and QSG0.5 films; these materials showed some of the best sorption capacities in the oil/water mixture. The results of the weight % loss at 135 °C could indicate that the use of antioxidants from cranberry, beetroot, pitaya, and grape (anthocyanins, betalains, and resveratrol) confers more thermal stability to the chitosan–starch films than thymol and carvacrol from oregano; these results are consistent with former research [25]. Jing et al. (2018) [33] found that the addition of phenolic compounds could reduce the thermal stability of chitosan conjugates, probably because of antioxidants (proanthocyanidins) obstructing the chitosan chain packing without affecting their practical applications. This statement could be related to the increment of weight loss of QSA0.5, QSG0.5, QSO0.5, and QSR0.5, where the quantity and type of phenolic compounds have influence, but do not affect the better oil sorption capacity in comparison with control film QS2, in most of the cases (see Table 3). The thermal stability was affected by the reduction of the extract concentration and the decrement of the phenolic compounds content [25].

**Figure 6.** Thermograms of QS2, Am0.5, QSA0.5, QSB0.5, QG0.5, QSO0.5, QSP0.5, and QSR0.5 films.

### 3.6. Apparent Density

The apparent density is inversely proportional to the porosity of the materials. The apparent density results are indicated in Table 7. The addition of extracts to the chitosan–starch films increase their apparent density, except for QSA0.5, QSO2, and QSR2.



**Table 7.** Apparent density of films.

Sample	Average Apparent Density (g/cm <sup>3</sup> )
QS2	0.0445 ± 0.0032
QSA0.5	0.0730 ± 0.0049
QSA2	0.0575 ± 0.0035
QSA0.5	0.0465 ± 0.0019
QSA0.2	0.0432 ± 0.0030
QSB0.5	0.0511 ± 0.0057
QSB2	0.0610 ± 0.0026
QSG0.5	0.0653 ± 0.0090
QSG2	0.0541 ± 0.0028
QSO0.5	0.0506 ± 0.0088
QSO2	0.0405 ± 0.0050
QSP0.5	0.0528 ± 0.0086
QSP2	0.0673 ± 0.0063
QSR0.5	0.0484 ± 0.0046
QSR2	0.0361 ± 0.0019

According to Ahmed et al. (2016) [16], the apparent density variation is due to different concentrations, the type of components, and the changes of porosity. It was observed that the films with a lower apparent density present the same behavior—a lower sorption capacity than QS2 in the presence of connate water, and higher than QS2 in the presence of deionized water and seawater. For the oil removal application, the films with a higher apparent density are the most recommended [21,25,32–35].

#### 4. Conclusions

Chitosan–starch films modified with natural extracts are biodegradable; with an easy synthesis and methodology. They presented potential oil spill applications, as evidenced by the tests carried out in this work.

- The modified materials with natural extracts quickly and efficiently removed heavy crude oil from connate water, deionized water, and seawater. The highest oil sorption capacity was observed in the oil/seawater mixture at the lowest extract concentration, which means that the maximum efficiency of films is reached, with cost reduction (using less extract quantity).
- The use of an extract with polyphenols, such as anthocyanins and betalains, enhances this capacity and increases the apparent density without affecting it. This can be observed in the increment of the surface area and pore volume of QSA0.5, in Appendix A.1.
- The highest global oil sorption capacity (in the three types of mixture—oil/connate water, oil/deionized water, and oil/seawater) was presented by the films with the lowest concentration of extracts (0.5% *v/v*), as follows: QSA0.5 > QSP0.5 > QSA0.5 > QSB0.5 > QSR0.5 > QSO0.5 > QSG0.5.
- Almost all of the modified materials, especially at 0.5% *v/v*, presented a competitive performance as a sorbent in comparison with the new green sorbents synthesized with chitosan, alginate, cellulose, etc. (please see Section 3.3, Removal of Heavy Oil from Connate Water/Deionized/Seawater Mixtures).
- The improvement of the sorption capacity is due to the hydrophobic interaction between the chitosan and antioxidants (polyphenols), which increment the affinity with oil.
- The heterogeneity of the film's morphology enhances the sorption capacity. The films with higher values presented more concavities and streaks on the film's surface in comparison with the other analyzed materials.
- The increment of the oil sorption capacity was confirmed by the GC–MS results of QSA2, where a higher volatile crude sorption was observed in comparison with the QS2 chromatogram.

- The film QSA0.5 showed the lowest weight loss at 130 °C (at that temperature, the extract's antioxidants present degradation). This implies that the presence of cranberry extract not only increases the sorption capacity, but also the thermal stability.
- An enhancement in thermal stability is shown in most of the films, related to the presence of extracts.

These results encourage further research in order to synthesize and apply these materials for the remedy of oil spills, especially in seawater and deionized (potable) water, because of their efficiency, suitable physical, thermal properties, lower-cost, and easy synthesis.

**\* Note 1:** The reduction of the synthesis cost is related to the simpler and greener way of obtaining of extracts, without using solvents such as ethanol or methanol, extraction methodology (Soxhlet or similar), less extract obtaining time, etc.

**\* Note 2:** The authors synthesized modified chitosan–starch films with 0.5%, 2%, and 5% extract concentrations. As a result of the poorest performance, such as the oil sorbent materials presented by films at 5%, these were eliminated in order to ease the information presentation.

**Author Contributions:** J.A.M.-B., N.P.D.-Z. and C.V.-S. designed the experiments and wrote the paper, together with J.I.L.-N., who also performed the experiments; F.P.-D. and J.F.P.-S. performed the films characterization; J.M.D.-E. and E.J.S.-D. analyzed the data; J.E.S.-S. revised written translation. All authors have read and agreed to the published version of the manuscript.

**Funding:** We would like to acknowledge the Secretaría de Energía (SENER)-Consejo Nacional de Ciencia y Tecnología (CONACyT) for the postdoctoral scholarship to Jessica I. Lozano-Navarro through project no. 177007, for the reagents and materials provided by TecNM 5502.19-P, and for the chromatographic analyses with autosampler model Turbomatrix 40 head space through the infrastructure project no. 295494.

**Conflicts of Interest:** The authors declare no conflict of interest.

## Appendix A

### Appendix A.1 Determination of Surface Area by the BET Method

The area of the actual surface and the pore volume of QSA0.5 were determinate to understand their relationship with the films' sorption capacity. This sample was analyzed because of its good behavior in the sorption capacity, and the enhanced physical properties in comparison with the control film to the known effect of the extract on some porous and surface properties.

The specific surface area was determined from the adsorption–desorption isotherm of nitrogen ( $N_2$ ) at  $-196$  °C (77 °K) in an analyzer model Quantachrome Autosorb Automated Gas Sorption System, brand Quantachrome Instruments (Boynton Beach, FL, USA), using the Brunauer Emmett Teller (BET) method.

In Table A1, the QS2 and QSA0.5 surface area and cumulative pore volume are shown. The addition of extracts from cranberry derived in an increment of surface area (from 21.51 to 97.734  $m^2/g$ ) and cumulative pore volume (35.89 from to 106.8  $cm^3/g$ ) are shown. This situation allows for a better oil sorption capacity in comparison with control film QS2 (see Table 3) [36].

**Table A1.** Brunauer Emmett Teller (BET) and Barrett, Joyner, and Halenda (BJH) summary report for QS2 and QSA0.5.

Characteristic	QS2	QSA0.5
$S_{BET}$ ( $m^2/g$ )	$21.51 \pm 1.21$	$97.734 \pm 2.20$
BJH desorption cumulative pore volume ( $cm^3/g$ )	$35.89 \pm 1.26$	$106.8 \pm 4.62$

The  $N_2$  adsorption–desorption isotherm of QSA0.5 is indicated in Figure A1. According to Sing et al. (1985), the isotherm curve is classified as type IV with hysteresis H4 [37].

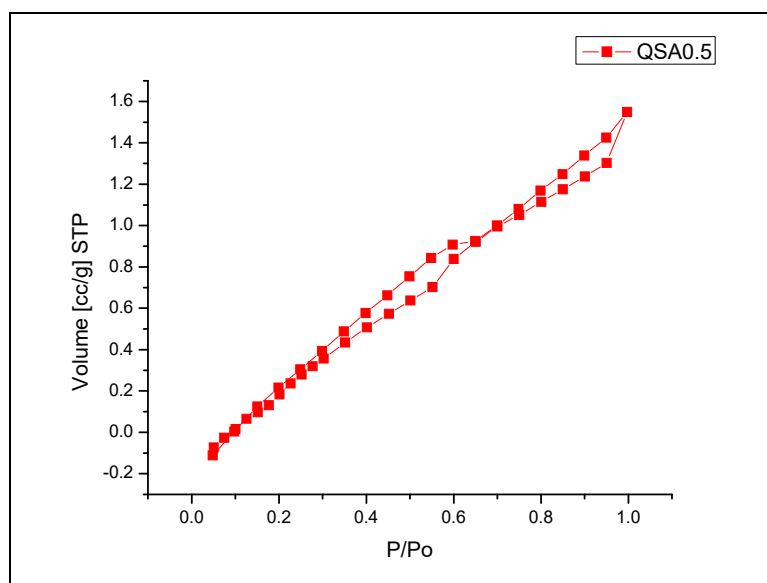


**Figure A1.** Nitrogen adsorption–desorption isotherm of QSA0.5.

#### Appendix A.2 Gas Chromatography–Mass Spectrometry (GC-MS)

The separation, isolation, and identification of volatile active compounds of modified films were carried out by gas chromatography–mass spectrometry analysis. These studies were performed on a GC–MS system model Clarus A600S, brand Perkin Elmer (Waltham, MA, USA), and an autosampler model Turbomatrix40 head space, brand Perkin Elmer (Waltham, MA, USA). For the analysis, 50 microliters of cranberry extract and 20 mg of the film sample with and without crude oil were used. For the separation of analytes, an Elite-624 column was used. Helium with a 99.9995% purity (Praxair, Tampico, Mexico), with a flow rate of 0.8 mL/min, was used as a carrier gas. The oven temperature was maintained at 40 °C for 1 min after injection, and then programmed at 8 °C/min to 220 °C, at which the column was maintained for 1 min. The split ratio was 10:1 for the extract analysis and 100:1 for the film analyses. The mass detector electron ionization was 70 eV. The data acquisition and processing were performed using the Perkin Elmer Turbomass Version 6.1.0 software (Waltham, MA, USA). The identification of the volatile compounds was carried out using mass spectra library search (NIST 2018), and comparing it with the mass spectral data from the literature. The film QSA2 presented the highest sorption capacity in all of the tests (24.98 oil/deionized water), because of this fact, the sample was analyzed in comparison with QS2 in order to confirm the higher oil sorption capacity.

The cranberry (*Vaccinium oxycoccus*) extract was analyzed by the GC–MS technique in order to determine its volatile constituents, percentage composition, and retention time. Through the GC–MS chemical composition analyses, 24 constituents were identified, corresponding to 100% of the volatiles from the cranberry extract. The main constituents were glycerin (30.8297%), 2-furancarboxylic hydrazide acid (19.4128%), 5-hydroxy methyl furfural (17.0169%), furfural (10.1282%), 2,3-dihydro-3,5-dihydroxy-6-methyl-4H-pyran-4-one (6.8816%), and alanine (3.0312%). These data are presented in Table A2.

**Table A2.** Constituents identified in cranberry extract.

Constituents	Retention Time (min)	%
Alanine (C <sub>3</sub> H <sub>7</sub> NO <sub>2</sub> )	1.81	3.0312
Methylphosphine* (CH <sub>5</sub> P)	4.74	0.2011
Acetic acid (CH <sub>3</sub> COOH)	5.04	0.3793
Methyloxirane* (C <sub>3</sub> H <sub>6</sub> O)	5.16	0.2799
Acetic acid methyl ester (C <sub>4</sub> H <sub>8</sub> O <sub>2</sub> )	5.54	0.2809
Propanedioic acid (C <sub>3</sub> H <sub>4</sub> O <sub>4</sub> )	5.87	0.1989
1-Methylpyrrolidin-3-amine (C <sub>5</sub> H <sub>12</sub> N <sub>2</sub> )	6.34	0.1565
1-Hydroxy-2-propanone (C <sub>3</sub> H <sub>6</sub> O <sub>2</sub> )	6.89	0.1834
Propanedioic acid, oxo-, bis(1-methylethyl) ester (C <sub>9</sub> H <sub>14</sub> O <sub>5</sub> )	8.69	0.1968
Furfural (C <sub>5</sub> H <sub>4</sub> O <sub>2</sub> )	10.17	10.1282
5-Methyl-2(3H)-furanone (C <sub>5</sub> H <sub>6</sub> O <sub>2</sub> )	11.12	1.0808
Glycerin (C <sub>3</sub> H <sub>8</sub> O <sub>3</sub> )	12.64	30.8297
2,4-Diethoxy-2,5-dimethyl-3 (2H) -furan-3-one (C <sub>14</sub> H <sub>18</sub> O <sub>3</sub> )	12.79	2.1231
5-Methyl-2-furancarboxaldehyde (C <sub>6</sub> H <sub>6</sub> O <sub>2</sub> )	13.19	1.1993
5-Methyl-2(5H)-furanone (C <sub>5</sub> H <sub>6</sub> O <sub>2</sub> )	13.64	1.0645
2-Furancarboxylic hydrazide acid	16.17	19.4128
4-oxopentanoic acid (C <sub>5</sub> H <sub>8</sub> O <sub>3</sub> )	16.37	0.3284
Levogluconenone (C <sub>6</sub> H <sub>6</sub> O <sub>3</sub> )	17.17	1.7384
2,3-Dihydro-3,5-dihydroxy-6-methyl-4H-pyran-4-one	17.34	6.8816
Benzoic acid (C <sub>7</sub> H <sub>6</sub> O <sub>2</sub> )	18.02	0.5578
N-methyl-N-nitroso-2-propanamine* (C <sub>4</sub> H <sub>10</sub> N <sub>2</sub> O)	18.77	0.2166
5-Acetoxymethyl-2-furaldehyde (C <sub>8</sub> H <sub>8</sub> O <sub>4</sub> )	19.09	1.9395
5-Hydroxy methyl furfural (C <sub>6</sub> H <sub>6</sub> O <sub>3</sub> )	19.97	17.0169
2,4-Dimethyl-2,6-heptadienal* (C <sub>9</sub> H <sub>14</sub> O)	22.37	0.5743
Total identified		100

\* <80% correspondence with the National Institute of Standards and Technology (NIST) library.

According to Garrido Conejero (2014), alanine is an amino acid present in the nutritional composition of cranberry [38]. The methylphosphine is an alternative fumigant with garlic-metallic odor [39]. Acetic acid and benzoic acid are carboxylic acids present in cranberry juice [40]. Methyloxirane, known as propylene oxide, is used as an alternative antimicrobial agent in food [41]. Propanedioic acid, known as malonic acid, is a carboxylic acid found in fruits [42]. Furfural is naturally present in cranberry as a trace, its derivatives contribute to the fruity and aromatic odor and flavor of cranberry juice [43]. 1-Hydroxy-2-propanone is a synthetic flavoring [44]. Glycerin or glycerol is a controversial and common substitute of sugar used in commercial cranberry juice, and keeps the moisture of the product [45]. 5-Methyl-2(3H)-furanone, 5-Methyl-2(5H)-furanone, and 5-Methyl-2-furancarboxaldehyde (the last is a product from saccharides) are flavoring agents. 4-oxopentanoic acid, known as levulinic acid, is a plant metabolite [46]. Levogluconenone is a compound obtained from the synthesis of biologically active products, and it is used in the chemical and pharmaceutical industry [47]. 5-Acetoxymethyl-2-furaldehyde is a natural substance and extract used because of its organoleptic properties [48]. The cranberry volatile compounds enhance the oil sorption because of their hydrophobic groups such as carboxylic acids (-ic), aldehydes (-al), cetones (-one), and alanine (amino acid).

In Figure A2, the chromatograms of heavy crude oil, QS2 film, and QSA2 film after the oil sorption process are presented. It was observed that both films show a sorption capacity of the oil's most volatile fractions, and the QSA2 film has a higher capacity in comparison with QS2 (inferring a higher relative abundance of ions in QSA2 vs. QS2). Figure A3 compares the chromatograms of each film before and after the oil sorption tests. The presence of signals in the samples after the sorption capacity test was clearly observed, which correspond with the crude oil chromatograms and confirm that the sorption phenomena occurred in both films, especially in the case of QSA2. This implies that the addition of cranberry extract significantly enhanced the sorption capacity, and can be attributed to the extract compounds such as carboxylic acids, antioxidants, and amino acids.

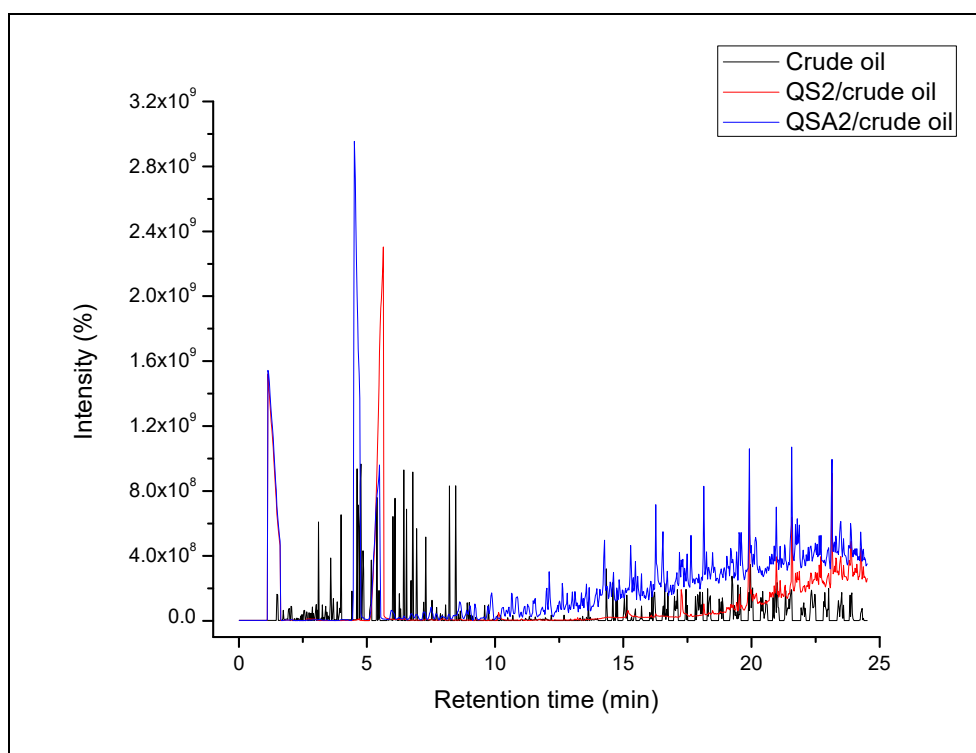


**Figure A2.** GC–MS chromatogram of heavy crude oil, and QS2 and QSA2 films after oil sorption.

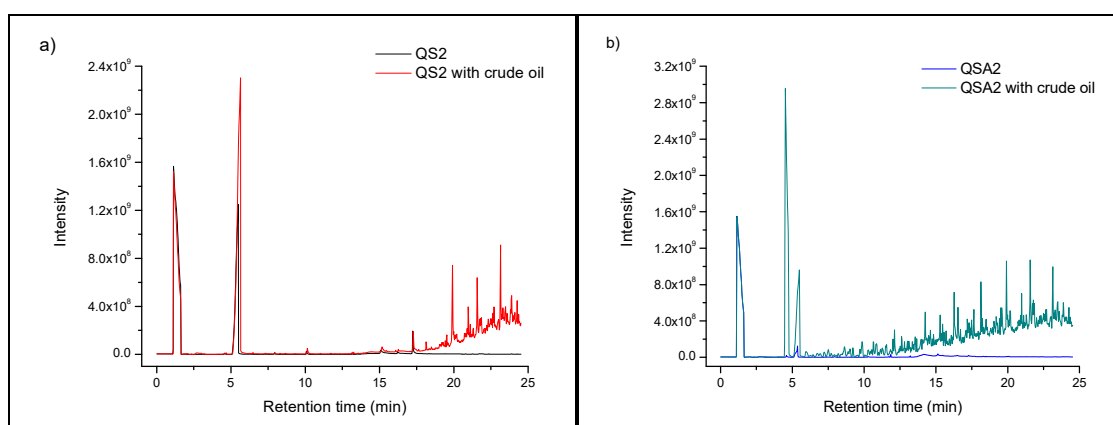


**Figure A3.** GC–MS comparative chromatogram of the (a) QS2 and (b) QSA2 films before and after oil sorption.

## References

1. Viswanathan, B. Chapter 2—Petroleum. In *Energy Sources Fundamentals of Chemical Conversion Processes and Applications*; Elsevier: Oxford, UK, 2017; pp. 29–57. [\[CrossRef\]](#)
2. Li, Z.; Shao, L.; Hu, W.; Zheng, T.; Lu, L.; Cao, Y.; Chen, Y. Excellent reusable chitosan/cellulose aerogel as an oil and organic solvent absorbent. *Carbohydr. Polym.* **2018**, *191*, 183–190. [\[CrossRef\]](#)
3. Liu, J.; Li, P.; Chen, L.; Feng, Y.; He, W.; Yan, X.; Lu, X. Superhydrophilic and underwater superoleophobic modified chitosan-coated mesh for oil/water separation. *Surf. Coat. Tech.* **2016**, *307*, 171–176. [\[CrossRef\]](#)
4. Ren, L.; Yan, X.; Zhou, J.; Tong, J.; Su, X. Influence of chitosan concentration on mechanical and barrier properties of corn starch/chitosan films. *Int. J. Biol. Macromol.* **2017**, *105*, 1636–1643. [\[CrossRef\]](#)
5. Doshi, B.; Eveliina Repo, E.; Heiskanen, J.P.; Sirviö, J.A.; Sillanpää, M. Effectiveness of N,O-carboxymethyl chitosan on destabilization of Marine Diesel, Diesel and Marine-2T oil for oil spill treatment. *Carbohydr. Polym.* **2017**, *167*, 326–336. [\[CrossRef\]](#)



6. Luo, Q.; Huang, X.; Gao, F.; Dong Li, D.; Wu, M. Preparation and Characterization of High Amylose Corn Starch–Microcrystalline Cellulose Aerogel with High Absorption. *Materials* **2019**, *12*, 1420. [[CrossRef](#)]
7. Long, L.-Y.; Li, F.-F.; Weng, Y.-X.; Wang, Y.-Z. Effects of Sodium Montmorillonite on the Preparation and Properties of Cellulose Aerogels. *Polymer* **2019**, *11*, 415. [[CrossRef](#)]
8. Wang, Y.; Feng, Y.; Yao, J. Construction of hydrophobic alginate-based foams induced by zirconium ions for oil and organic solvent cleanup. *J. Colloid Interface Sci.* **2019**, *533*, 182–189. [[CrossRef](#)]
9. Ocampo, R.; Ríos, L.A.; Betancur, L.A.; Ocampo, D.M. *Curso Práctico de Química Orgánica Enfocado a Biología y Alimentos*, 1st ed.; Editorial Universidad de Caldas: Manizales, Colombia, 2008.
10. Marañón-Ruiz, V.F.; Rizo de la Torre, L.D.C. Caracterización de las propiedades ópticas de Betacianinas y Betaxantinas por espectroscopía UV–VIS y barrido en Z. *Superficies y Vacío* **2011**, *24*, 113–120.
11. García-García, R.M.; Palou-García, E. Mecanismos de acción antimicrobiana de timol y carvacrol sobre microorganismos de interés en alimentos. *Temas Selectos de Ingeniería de Alimentos* **2008**, *2*, 41–51.
12. Gambini, J.; López-Grueso, R.; Olaso-González, G.; Inglés, M.; Abdelazida, K.; El-Alami, M.; Bonet-Costa, V.; Borrás, C.; Viña, J. Resveratrol: Distribución, propiedades y perspectivas. *Revista Española de Geriatría y Gerontología* **2013**, *48*, 79–88. [[CrossRef](#)]
13. Lozano-Navarro, J.I.; Díaz-Zavala, N.P.; Velasco-Santos, C.; Martínez-Hernández, A.L.; Tijerina-Ramos, B.I.; García-Hernández, M.; Rivera-Armenta, J.L.; Páramo-García, U.; Reyes-de la Torre, A.I. Antimicrobial, Optical and Mechanical Properties of Chitosan–Starch Films with Natural Extracts, International. *Int. J. Mol. Sci.* **2017**, *18*, 997. [[CrossRef](#)] [[PubMed](#)]
14. Souza, V.G.L.; Fernando, A.L.; Pires, J.R.A.; Rodrigues, P.F.; Lopes, A.A.; Fernandes, F.M.B. Physical properties of chitosan films incorporated with natural antioxidants. *Ind. Crops Prod.* **2017**, *107*, 565–572. [[CrossRef](#)]
15. Tsao, R. Chemistry and Biochemistry of Dietary Polyphenols. *Nutrients* **2010**, *2*, 1231–1246. [[CrossRef](#)]
16. Ahmed, S.; Ikram, S. Chitosan and gelatin based biodegradable packaging films with UV-light protection. *J. Photochem. Photobiol. B* **2016**, *163*, 115–124. [[CrossRef](#)]
17. Pastor, C.; Sánchez-González, L.; Chiralt, A.; Cháfer, M.; González-Martínez, C. Physical and antioxidant properties of chitosan and methylcellulose based films containing resveratrol. *Food Hydrocoll.* **2013**, *30*, 272–280. [[CrossRef](#)]
18. Wang, L.; Dong, Y.; Men, H.; Tong, J.; Zhou, J. Preparation and characterization of active films based on chitosan incorporated tea polyphenols. *Food Hydrocoll.* **2013**, *32*, 35–41. [[CrossRef](#)]
19. Blanquicet-Macea, R.; Flórez de Hoyos, C.; González Montes, Y.; Meza Fuentes, E.; Rodríguez Ruíz, J.I. Síntesis y propiedades de polímeros basados en quitosano/lactosuero. *Polímeros Ciencia e Tecnología* **2015**, *25*, 58–69. [[CrossRef](#)]
20. Mayachiew, P.; Devahastin, S. Effects of drying methods and conditions on release characteristics of edible chitosan films enriched with Indian gooseberry extract. *Food Chem.* **2010**, *118*, 594–601. [[CrossRef](#)]
21. Park, S.Y.; Marsh, K.S.; Rhim, J.W. Characteristics of Different Molecular Weight Chitosan Films Affected by the Type of Organic Solvents. *Food Eng. Phys. Prop.* **2012**, *67*, 194–197. [[CrossRef](#)]
22. Saruchi, S.; Kumar, V.; Vikas, P.; Kumar, R.; Kumar, B.; Kaur, M. Low cost natural polysaccharide and vinyl monomer based IPN for the removal of crude oil from water. *J. Petrol. Sci. Eng.* **2016**, *141*, 1–8. [[CrossRef](#)]
23. Rongsayamanont, W.; Soonglerdsongpha, S.; Khondee, N.; Pinyakong, O.; Tongcumpou, C.; Sabatini, D.A.; Luepromchai, E. Formulation of crude oil spill dispersants based on the HLD concept and using a lipopeptide biosurfactant. *J. Hazard Mater.* **2017**, *334*, 168–177. [[CrossRef](#)] [[PubMed](#)]
24. Elanchezhian, S.S.D.; Meenakshi, S. Synthesis and characterization of chitosan/Mg–Al layered double hydroxide composite for the removal of oil particles from oil-in-water emulsion. *Int. J. Biol. Macromol.* **2017**, *104*, 1586–1595. [[CrossRef](#)] [[PubMed](#)]
25. Lozano-Navarro, J.I.; Díaz-Zavala, N.P.; Velasco-Santos, C.; Melo-Banda, J.A.; Páramo-García, U.; Paraguay-Delgado, F.; García-Alamilla, R.; Martínez-Hernández, A.L.; Zapién-Castillo, S. Chitosan–Starch Films with Natural Extracts: Physical, Chemical, Morphological and Thermal Properties. *Materials* **2018**, *11*, 120. [[CrossRef](#)]
26. Doshi, B.; Repo, E.; Heiskanen, J.P.; Sirvi, J.A.; Sillanp, M. Sodium salt of oleoyl carboxymethyl chitosan: A sustainable adsorbent in the oil spill treatment. *J. Clean. Prod.* **2018**, *170*, 339–350. [[CrossRef](#)]

27. Noshirvani, N.; Ghanbarzadeh, B.; Gardrat, C.; Rezaei, M.R.; Le Coz, C.; Coma, V. Cinnamon and ginger essential oils to improve antifungal, physical and mechanical properties of chitosan-carboxymethyl cellulose films. *Food Hydrocoll.* **2017**, *70*, 36–45. [CrossRef]
28. Martínez-Camacho, A.P.; Cortez-Rocha, M.O.; Ezquerro-Brauer, J.M.; Graciano-Verdugo, A.Z.; Rodríguez-Félix, F.; Castillo-Ortega, M.M.; Yépiz-Gómez, M.S.; Plascencia-Jatomea, M. Chitosan composite films: Thermal, structural, mechanical and antifungal properties. *Carbohydr. Polym.* **2010**, *82*, 305–315. [CrossRef]
29. Mina, J.; Valadez-González, A.; Herrera-Franco, P.; Delvasto, S. Caracterización fisicoquímica del almidón termoplástico de yuca natural y acetilada. *Univ. Nac. Colomb. Med.* **2011**, *78*, 166–173. [CrossRef]
30. Benavides Rodríguez, L.; Sibaja Ballester, M.; Vega-Baudrit, J.; Camacho Elizondo, M.; Madrigal Carballo, S. Estudio Cinético de la degradación térmica de Quitina y Quitosano de camarón de la especie “*Heterocarpus Vicarius*” empleando la técnica termogravimétrica en modo dinámico. *Revista Iberoamericana de Polímeros* **2010**, *11*, 561–562.
31. Yang, D.; Li, J.; Jiang, Z.; Lu, L.; Chen, X. Chitosan/TiO nanocomposite pervaporation membranes for ethanol dehydration. *Chem. Eng. Sci.* **2009**, *64*, 3130–3137. [CrossRef]
32. O’Neil, M.J.; Heckelman, P.E.; Koch, C.B.; Roman, K.J. *The Merck Index—An Encyclopedia of Chemicals, Drugs, and Biologicals*; Merck and Co.: Whitehouse Station, NJ, USA, 2006.
33. Jing, Y.; Huang, J.; Yu, X. Preparation, characterization, and functional evaluation of proanthocyanidin-chitosan conjugate. *Carbohydr. Polym.* **2018**, *194*, 139–145. [CrossRef]
34. Porosidad y Permeabilidad. Available online: [https://pendientedemigracion.ucm.es/info/diciex/proyectos/agua/esc\\_sub\\_porosidad.html](https://pendientedemigracion.ucm.es/info/diciex/proyectos/agua/esc_sub_porosidad.html) (accessed on 5 March 2019).
35. Densidad Aparente. Available online: <http://araucarias.blogspot.mx/2005/09/densidadaparente.html> (accessed on 5 March 2019).
36. Dos Santos, J.M.N.; Pereira, C.R.; Foletto, E.L.; Dotto, G.L. Alternative synthesis for ZnFe<sub>2</sub>O<sub>4</sub>/chitosan magnetic particles to remove diclofenac from water by adsorption. *Int. J. Biol. Macromol.* **2019**, *131*, 301–308. [CrossRef] [PubMed]
37. Sing, K.S.W.; Everett, D.H.; Haul, R.A.W.; Moscou, L.; Pierotti, R.A.; Rouquerol, J.; Siemieniewska, T. Reporting physisorption data for gas/solid systems with special reference to the determination of surface area and porosity. *Pure Appl. Chem.* **1985**, *57*, 603–619. [CrossRef]
38. Garrido Conejero, M.V.; Pérez-Urria, E. Arándano Rojo I (*Vaccinium macrocarpon* Ait.). *REDUCA (Biología)* **2014**, *7*, 100–112.
39. Chaudhry, M.Q.; MacNicoll, A.D.; Mills, K.A.; Price, N.R. The potential of methylphosphine as a fumigant for the control of phosphine-resistant strains of four species of stored product insects. In Proceedings of the International Conference on Controlled Atmosphere and Fumigation in Stored Products, Nicosia, Cyprus, 21–26 April 1996; pp. 45–57.
40. Isham, P.D. The Acids of the Cranberry. Ph.D. Thesis, University of Massachusetts, Amherst, MA, USA, 1935; p. 903.
41. Oyarzabal, O.A.; Backert, S. *Microbial Food Safety: An Introduction*; Springer Science & Business Media: Berlin/Heidelberg, Germany, 2011.
42. Duarte, A.M.; Caixeirinho, D.; Miguel, M.G.; Sustelo, V.; Nunes, C.; Fernandes, M.M.; Marreiros, A. Organic acids concentration in citrus juice from conventional versus organic farming. *Acta Hort.* **2012**, *933*, 601–606. [CrossRef]
43. Mills, S.; Bone, K. *The Essential Guide to Herbal Safety*; Elsevier Health Sciences: Amsterdam, The Netherlands, 2005.
44. Synthetic Flavoring Substances. Available online: <https://www.foodsafetykorea.go.kr/foodcode/pdf/2/2-4/613.pdf> (accessed on 26 March 2019).
45. Why We No Longer Recommend ‘Reduced Sugar’ Cranberries. Available online: [https://medium.com/@chuck\\_ehrlich/why-we-no-longer-recommend-reduced-sugar-cranberries-8d484cf7a24](https://medium.com/@chuck_ehrlich/why-we-no-longer-recommend-reduced-sugar-cranberries-8d484cf7a24) (accessed on 26 March 2019).
46. 5-Methyl-2(3H)-Furanone. Available online: [https://pubchem.ncbi.nlm.nih.gov/compound/alpha-Angelica\\_lactone](https://pubchem.ncbi.nlm.nih.gov/compound/alpha-Angelica_lactone) (accessed on 26 March 2019).

47. Pandey, A.; Bhaskar, T.; Stöcker, M.; Sukumaran, R. *Recent Advances in Thermo-Chemical Conversion of Biomass*; Elsevier: Amsterdam, The Netherlands, 2015; pp. 75–108.
48. 5-Acetoxymethyl-2-Furaldehyde. Available online: <http://www.thegoodscentscompany.com/data/rw1208491.html> (accessed on 26 March 2019).



© 2019 by the authors. Licensee MDPI, Basel, Switzerland. This article is an open access article distributed under the terms and conditions of the Creative Commons Attribution (CC BY) license (<http://creativecommons.org/licenses/by/4.0/>).